ACS OMEGA

http://pubs.acs.org/journal/acsodf

Article

Nanoencapsulated Extract of a Red Seaweed (Rhodophyta) Species as a Promising Source of Natural Antioxidants

Yasmin R. Maghraby,* Mohamed A. Farag, Michael G Kontominas, Zeinab T. Shakour, and Adham R. Ramadan

Cite This: *ACS Omega* 2022, 7, 6539–6548

Read Online

ACCESS | Metrics & More | Article Recommendations | Supporting Information

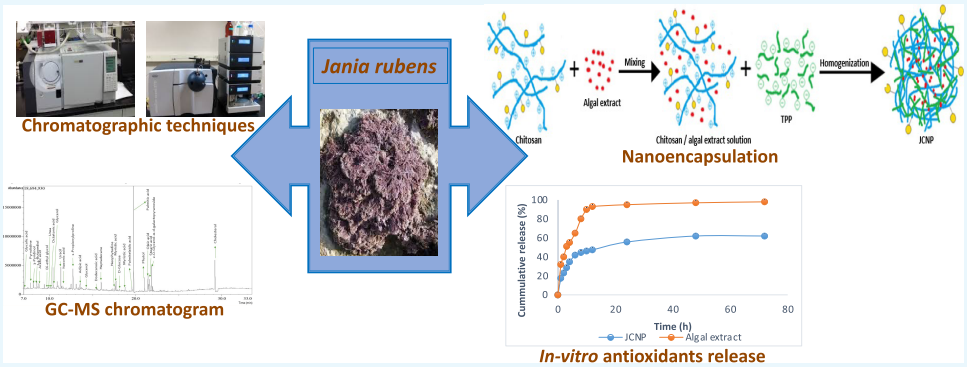

ABSTRACT: Marine seaweed species represent an important source of bioactive compounds possessing antioxidant activity. This study aimed at evaluating the antioxidant capacity of the *Jania rubens* algal extract by means of two antioxidant assays, i.e., 2,2-diphenyl-1-picrylhydrazyl and ferric-reducing antioxidant power. The seaweeds' total phenolic and flavonoid contents were also assayed as markers of antioxidant activity. To identify active agents responsible for the antioxidant activity, gas chromatography-mass spectrometry and liquid chromatography-mass spectrometry were used for comprehensive metabolites characterization. To enhance the *Jania rubens* efficacy, the extract was nanoencapsulated using an ionic gelation method by means of high-pressure homogenization. The optimum nanoformulation had a particle size of 161 nm, a ζ potential of 31.2 mV, a polydispersity index of 0.211, and entrapment efficiency of 99.7%. The *in vitro* phytochemicals' release profiles of *Jania rubens* chitosan nanoparticles in comparison to the concentration of the raw algal extract were studied by the dialysis bag diffusion method revealing that the extract was released in a controlled pattern. The results indicated the potential advantages of the encapsulated *Jania rubens* extract, with its potent antioxidant activity, for use in different applications where sustained release is useful.

1. INTRODUCTION

Antioxidants provide protection to humans against many degenerative diseases through their radical scavenging activity.[1] The development of natural antioxidants that can substitute the synthetic counterparts is a modern trend that most consumers prefer. Natural antioxidants can block the oxidation reactions that produce different types of free radicals that cause damage to living cells. Natural antioxidants are thus useful for the human body and can be used in different applications such as pharmaceuticals, foods and beverages, medicinal and cosmetic products, etc.[2] Several antioxidants have been extracted and used from natural terrestrial plants, but there has been less emphasis on marine seaweeds. Marine algal species represent an important source of bioactive compounds possessing antioxidant activity. Besides being a good source of antioxidants (β-carotene and polyphenols),[3] seaweeds are abundant in minerals (Ca, P, Na, K, Mg, and Na)[4] and vitamins (A, B_1, B_{12}, C, D, E, etc.).[5]

Jania rubens (*J. rubens*), a red (rhodophyta) Mediterranean seaweed species found along the coast of Alexandria [Egypt][6] is rich in many phytochemicals including polyphenols and diterpenes,[7] with the major classes of polyphenols being flavonoids and tannins.[8] Phytochemicals that can be derived from *J. rubens* can be used as additives in food products, supplements, and cosmetics.[9]

The health benefits of phytochemicals inside the human body depend on their bioavailability.[10] A formulation that maintains the structural integrity and improves the bioavailability of the phytochemicals after ingestion is needed as a

Received: October 4, 2021
Accepted: February 4, 2022
Published: February 16, 2022

https://doi.org/10.1021/acsomega.1c05517
ACS Omega 2022, 7, 6539–6548

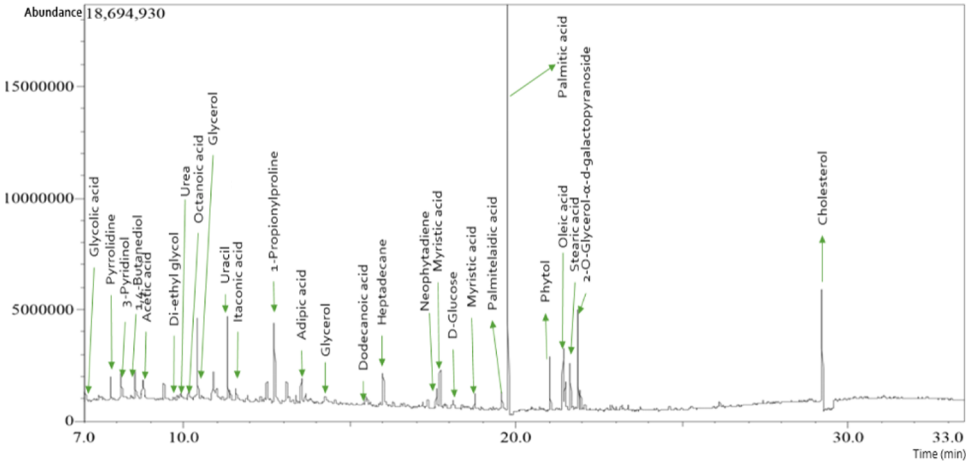

Figure 1. GC-MS chromatogram of the *J. rubens* ethanol extract.

small portion of the plant/algal extracts administered orally are absorbed efficiently by the human body,[11] besides that their uptake is being limited to about 20%.[12] Furthermore, phytochemicals are unstable in the acidic and alkaline environments of the stomach and the small intestine, respectively, which leads to their degradation.[5,10]

Nanoencapsulation of the algal phytochemicals is an approach with the potential of overcoming the above limitations.[13] Nanocapsules protect the entrapped bioactive compounds from the different pH environments along the gastrointestinal tract and accordingly prevent the antioxidants' degradation.[12] Additionally, nanocapsules have the ability to prolong the phytochemicals' half-life by protecting them from undergoing extensive transformations that could take place along the harsh environments of the gastrointestinal tract.[10] Last, but not least, most nanocapsules' materials exhibit bioadhesion properties toward the intestinal epithelium mucus, facilitating the absorbtion of the algal antioxidants.[14]

The nanoencapsulating carrier material should be biodegradable/biocompatible and stable after ingestion.[15] The most suitable nanocarrier materials are the carbohydrate-based delivery systems as these possess a high potential to be modified to achieve the required properties. Carbohydrate-based delivery systems can interact with a wide range of phytochemicals via their functional groups, which makes them versatile carriers to entrap a variety of hydrophilic/hydrophobic bioactive compounds.[16] Chitosan (CS) is a natural polysaccharide and is one of the most commonly used delivery systems in diverse fields.[17] CS is used in the pharmaceutical, medicinal, and food industries owing to its general recognition as GRAS (generally recognized as safe) by the United States Food and Drug Administration.[18] Properties such as *in situ* gelation, biodegradability, biocompatibility, and nontoxicity make CS suitable for usage in pharmaceutical formulations and in food systems. Some reports indicate that an entire CS nanoparticle (NP) can be taken up by the human cells, significantly enhancing the bioavailability of the entrapped antioxidants and other algal secondary metabolites.[19]

The present study aimed at characterizing the phytochemical extract from *J. rubens* and encapsulating it in chitosan nanoparticles for a controlled release. Phytochemicals were extracted from the *J. rubens* matrices using ethanol. The extract was assayed for its antioxidant activity and analyzed for its chemical composition using chromatographic hyphenated techniques, i.e., gas chromatography-mass spectrometry (GC-MS) and liquid chromatography-mass spectrometry (LC-MS). *J. rubens* chitosan-tripolyphosphate nanoparticles (JCNP) were prepared by ionic gelation using sodium tripolyphosphate (TPP) as the cross-linking agent with the aim of protecting the entrapped bioactive compounds.[20] *In vitro* phytochemicals' release from the JCNP was determined by the dialysis bag diffusion method and compared with the raw algal extract.

2. RESULTS AND DISCUSSION

2.1. Total Phenolic/Flavonoid Contents and Antioxidant Assays. *2.1.1. Total Phenolic Content (TPC) and Total Flavonoid Content (TFC).* The TPC of *J. rubens* was calculated to be at 121.8 ± 0.1 mg GAE (gallic acid equivalents)/g dw, higher than that reported for the *J. rubens* methanol extract collected from the coast of India,[7] likely attributed to different extraction solvents or algal origins. In contrast, the TFC of the *J. rubens* extract was calculated to be 60.9 ± 0.26 mg QE (quercetin equivalents)/g dry extract and comparable to that obtained in previous reports for samples from Abu-Qir Bay (Alexandria, Egypt) at 40 mg QE/g.[21]

2.1.2. 2,2-Diphenyl-1-picrylhydrazyl (DPPH) and Ferric Reducing Antioxidant Power (FRAP) Assays. The change in % radical scavenging activity (RSA) and % remaining DPPH with different concentrations of the *J. rubens* extract is shown in Supporting Information Figure 1. The % RSA ranged from 10.3 to 50.2%. It was also evident that an increase in the extract dose increased the % RSA in a linear manner, suggestive of a potential free radical scavenging activity. The half-maximal scavenging concentration (SC50) value was calculated as 3.87 (mg/mL). Similar results were observed in the case of the FRAP assay with a half-maximal inhibitory concentration (IC_{50}) value of the *J. rubens* algal extract to be 46.84 ± 0.74 mg trolox/g dw.

2.2. *J. rubens* Metabolites' Analyses via Hyphenated Techniques. *2.2.1. GC-MS.* GC-MS was adopted for profiling of lyophilic or small molecular weight compounds responsible for *J. rubens*' antioxidant effect, as shown in Figure 1 and Table 1. A total of 45 chromatographic peaks were recorded, of which 38 were identified as fatty acids, terpenes, sterols, and nitrogenous compounds. The GC-MS analysis revealed an abundance of fatty acids, e.g., myristic acid, palmitelaidic acid, palmitic acid, heptadecanoic acid, dodecanoic acid, oleic acid, stearic acid, and arachidic acid, some of which are known to

https://doi.org/10.1021/acsomega.1c05517
ACS Omega 2022, 7, 6539−6548

Table 1. Phytochemicals Identified in the *J. rubens* Ethanol Extract Using GC-MS

peak no.	Rt[a] (min)	KI[b]	area	compound name	molecular formula
1	7.05	1084.7	1152	glycolic acid, 2TMS	$C_2H_4O_3$
2	8.61	1173.2	874	acetic acid	CH_3COOH
3	9.76	1242.2	1306	4-hydroxybutanoic acid	$C_4H_8O_3$
4	10.17	1268.8	1424	octanoic acid, TMS ester	$C_8H_{16}O_2$
5	11.57	1360.2	1782	itaconic acid, 2TMS	$C_5H_6O_4$
6	13.68	1512.6	897	adipic acid, 2TMS	$C_6H_{10}O_4$
7	14.27	1557.8	692	cinnamic acid	$C_9H_8O_2$
8	15.48	1654.6	714	dodecanoic acid, TMS	$C_{12}H_{24}O_2$
9	9.91	1252.2	1084	diethylene glycol, 2TMS	$C_4H_{10}O_3$
10	10.42	1285.6	7270	glycerol, 3TMS	$C_3H_8O_3$
11	7.47	1108.2	1182	3,4,5-trimethylheptane	$C_{10}H_{22}$
12	16.02	1699.8	3232	heptadecane	$C_{17}H_{36}$
13	15.41	1648.4	961	4-acetamido-1-phenylpyrazole	$C_{11}H_{11}N_3O$
14	17.72	1849.1	1591	myristic acid, TMS	$C_{14}H_{28}O_2$
15	18.77	1947.7	1334	myristic acid, TMS	$C_{14}H_{28}O_2$
16	19.58	2026.7	17204	palmitelaidic acid, TMS	$C_{18}H_{34}O_2$
17	19.77	2045.9	21646	palmitic acid, TMS	$C_{16}H_{32}O_2$
18	20.73	2144.8	452	heptadecanoic acid, TMS	$C_{17}H_{34}O_2$
19	21.43	2218.9	2416	oleic acid, TMS	$C_{18}H_{34}O_2$
20	21.49	2225.3	1744	oleic acid, TMS	$C_{18}H_{34}O_2$
21	21.64	2242.8	2637	stearic acid-TMS	$C_{18}H_{36}O_2$
22	23.37	2441.9	544	arachidic acid,TMS	$C_{20}H_{40}O_2$
23	10.90	1316.3	1353	unknown nitrogenous compound	
24	11.33	1344.7	4306	unknown nitrogenous compound	
25	11.41	1349.8	1069	uracil, 2TMS	$C_4H_4N_2O_2$
26	12.52	1425.0	1451	unknown nitrogenous compound	
27	12.74	1442.1	3221	1-propionylproline, TMS derivative	$C_8H_{13}NO_3$
28	13.55	1502.9	1156	unknown nitrogenous compound	
29	23.76	2491.6	498	unknown nitrogenous compound	
30	7.60	115.6	962	2-butyl-1-methylpyrrolidine	$C_9H_{19}N$
31	8.12	1144.6	3372	3-pyridinol, TMS	C_5H_5NO
32	8.77	1181.0	1996	3-hydroxypicolinic acid, 2TMS	$C_6H_5NO_3$
33	9.82	1246.4	1157	urea, 2TMS	CH_4N_2O
34	12.33	1411.2	757	phloroglucinol, O,O'-bis(trimethylsilyl)	$C_6H_6O_3$
35	14.56	1579.3	1004	unknown steroid, TMS	
36	21.95	2276.9	1209	unknown sterol, TMS	
37	29.22	3182.4	3529	cholesterol, TMS	$C_{27}H_{46}O$
38	19.34	2001.3	559	galactopyranose, 5TMS	$C_6H_{12}O_6$
39	21.88	2269.2	11343	O-glycerol-α-galactopyranoside	$C_{27}H_{66}O_8$
40	16.32	1726.1	566	levoglucosan, 3TMS	$C_6H_{10}O_5$
41	18.44	1916.8	470	D-glucose, 6 TMS	$C_6H_{12}O_6$
42	17.62	1839.6	670	neophytadiene	$C_{20}H_{38}$
43	17.90	1865.2	506	neophytadiene	$C_{20}H_{38}$
44	21.03	2176.3	6862	phytol, TMS derivative	$C_{20}H_{40}O$

[a]Retention time. [b]Kovats index.

exhibit antioxidant activity.[22−24] The identified short-chain organic acids and phenols included cinnamic acid, acetic acid, 4-hydroxybutanoic acid, etc., of which cinnamic acid, itaconic acid, adipic acid, and glycolic acid are known to exhibit a potent antioxidant activity.[25] Short-chain alcohols were also detected though at much lower levels, i.e., 1,4-butanediol, diethylene glycol, and glycerol, with glycerol functioning as a food preservative owing to its antioxidant activity.[26] Several nitrogenous compounds including uracil, 1-propionylproline, pyrrolidine, 2-butyl-1-methyl, 3-pyridinol, and 3-hydroxypicolinic acid were detected.[27] Other lypophilic metabolites identified with a potential antioxidant effect included phytol and neophytadiene. Phytol is used as antimicrobial, anti-inflammatory, antidiuretic, and immunostimulatory, asides from its potential antioxidant effect.[26]

2.2.2. LC-MS. Compared to GC-MS, LC-MS is a powerful technique in identifying polar and large molecular weight type metabolites that cannot be detected using GC-MS. Consequently, to provide a comprehensive metabolite coverage of *J. rubens*, the extract was also analyzed using LC-MS. A total of 13 chromatographic peaks were recorded corresponding to phenolic acids, amino acids, coumarins, and fatty acids (Table 2). Fatty acids were the most abundant groups in *J. rubens*, in agreement with GC/MS analysis, followed by phenolic acids identified in peaks 1, 3, 5, and 6 $(M-H)^-$ at m/z 200.961, 197.81, 165.95, and 277.91, respectively. Phenolic acids yield fragmentation patterns characterized by the loss of CO_2 (44 Da) from the carboxylic acid group as in peaks 3, 5, and 6. The product ion spectrum of the deprotonated peak at m/z 197.81 (Rt = 0.62 min) showed a base peak [M-OH-H]- at m/z 179 due to the cleavage of the water molecule and at m/z 153 [M-H-44], for the loss of CO_2. Other product ions were observed at m/z 168 $[M-H-30]^-$ due to the loss of the methoxy group and at m/z 138 due to the cleavage of a second methoxy group. Based on the above fragmentation pattern, peak 3 was annotated as syringic acid, a hydroxybenzoic acid with a C6-C1 configuration. Syringic acid is an antioxidant that has been previously used as an antioxidant agent.[28] Comparison of the fragmentation patterns of peaks 3 and 6 indicated that they were similar, except that compound 6 has more sulfate groups confirmed by the product ion peak at m/z 197$[M-SO3-H]^-$. Consequently, peak 6 was annotated as syringic acid sulfate.

The MS/MS spectrum pattern of peak 5 at m/z 165.95 exhibited a major product ion at m/z 133 due to the loss of two water molecules, and another diagnostic product ion at m/z 122 [M-H-44]-, characteristic of a benzoic acid moiety. Consequently, peak 5 was annotated as benzene dicarboxylic acid with potential antioxidant activity.[29] The precursor ion at m/z 272.96 [M-H]- in peak 2 showed a unique fragmentation at m/z 255, 237, 228, 214, 200, 187, and 159, characteristic of a coumarins' subclass. Previously, 6,7-dihydroxy coumarin-3-sulfate was isolated from the green algae *Dasycladus vermicularis*,[30] exhibiting a strong antioxidant activity[31] and likely contributing to the observed antioxidant effects of *J. rubens*.

Reports have revealed that phenolic compounds are the most effective antioxidants in red algae.[32] Antioxidant activity of marine algae has been reported in numerous species, including *Ahnfeltiopsis, Hydroclathrus, Padina, Polysiphonia*, and *Turbinaria*.[33] Carotenoids and phenolic compounds, directly or indirectly contributed to the inhibition or suppression of oxidation processes.[2]

Peak 4 at [M-H]- 187.10 (Rt: 10.54 min) showed fragment ions at 169 $[M-H_2O-H]-$, 142 [M-COO-H]−, and 126[M-COO-NH_2-H]−. Such a fragmentation pattern is consistent with that of laminine ($C_9H_{20}N_2O_2$) belonging to betaines. Betaines are a class of quaternary ammonium compounds

https://doi.org/10.1021/acsomega.1c05517
ACS Omega 2022, 7, 6539−6548

Table 2. Metabolites Identified via LC-MS in *J. rubens* in a Negative Ionization Mode

peak no.	Rt[a] (min)	[M-H]−	metabolite	MS^n ions (*m*/*z*)	molecular formula	error (ppm)	class
1	0.51	200.96	dihydroxyphenyl glycerol	183, 157, 110, 89	$C_9H_{11}O_5^-$	3.76	phenolic
2	0.51	272.96	dihydroxycoumarin sulfate	255,237, 228, 214, 200, 187	$C_9H_5O_8S^-$	5.78	coumarin
3	0.58	197.81	syringic acid	170, 168, 153, 135	$C_9H_9O_5^-$	2.76	phenolic
4	10.54	187.10	laminine	169, 160, 142, 125	$C_9H_{19}N_2O_2^-$	0.57	betaine
5	11.12	165.95	benzenedicarboxylic acid	133, 122	$C_8H_5O_4^-$	3.15	aromatic acid
6	11.86	277.91	syringic acid sulfate	197,165, 137	$C_9H_9O_8S^-$	0.26	phenolic
7	13.38	242.18	pentadecanoic acid	225, 198, 181	$C_{15}H_{29}O_2^-$	−1.63	fatty acid
8	14.89	323.22	hydroxyeicosadienoic acid	305, 279, 197, 183	$C_{20}H_{35}O_3^-$	2.81	fatty acid
9	16.57	265.15	heptadecadienoic acid	239, 221, 98	$C_{17}H_{29}O_2^-$	1.92	fatty acid
10	17.04	297.15	nonadecanoic acid	279, 253, 197, 183	$C_{19}H_{37}O_2^-$	0.62	fatty acid
11	17.53	311.17	arachidic acid	293, 267, 197, 183	$C_{20}H_{39}O_2^-$	1.73	fatty acid
12	18.61	325.18	arachidic acid methyl ester	296, 267, 225,197, 183	$C_{21}H_{41}O_2^-$	2.04	fatty acid
13	19.25	339.20	arachidic acid ethyl ester	311, 295, 239, 183	$C_{22}H_{43}O_2^-$	−0.9	fatty acid

[a]Retention time.

Table 3. Vaules of Dependent Variables[j]

formula	PS ± SD (%)	ZP ± SD (nm)	PDI ± SD	EE % ± SD
F1	338 ± 1.83^{f}	+28.4 ± 3.78^{ab}	0.140 ± 0.06^{e}	60 ± 9.76^{e}
F2	310 ± 3.97^{g}	+29.7 ± 1.75^{ab}	0.216 ± 0.01^{cd}	72 ± 6.39^{bcde}
F3	161 ± 2.87^{i}	+31.2 ± 0.87^{a}	0.211 ± 0.07^{cd}	97 ± 4.87^{a}
F4	401 ± 12.70^{c}	+28.6 ± 0.99^{ab}	0.214 ± 0.02^{c}	88 ± 3.09^{ab}
F5	495 ± 20.57^{b}	+28.9 ± 1.56^{ab}	0.196 ± 0.01^{cd}	87 ± 3.76^{abc}
F6	669 ± 6.43^{a}	+31.0 ± 1.73^{a}	0.376 ± 0.01^{a}	60 ± 8.64^{e}
F7	293 ± 0.97^{g}	+27.9 ± 3.10^{ab}	0.297 ± 0.02^{b}	74 ± 2.18^{bcde}
F8	312 ± 8.79^{g}	+29.7 ± 6.39^{ab}	0.139 ± 0.01^{e}	62 ± 3.76^{e}
F9	350 ± 5.98^{ef}	+28.8 ± 9.02^{ab}	0.174 ± 0.01^{cde}	71 ± 2.21^{cde}
F10	364 ± 3.95^{de}	+29.4 ± 3.89^{ab}	0.188 ± 0.03^{cde}	68 ± 8.43^{de}
F11	347 ± 7.93^{ef}	+29.2 ± 3.92^{ab}	0.161 ± 0.03^{de}	84 ± 2.48^{abcd}
F12	380 ± 1.69^{cd}	+17.0 ± 8.91^{b}	0.340 ± 0.01^{ab}	79 ± 8.40^{bcd}
F13	252 ± 0.85^{h}	+29.0 ± 3.22^{ab}	0.172 ± 0.02^{cde}	61 ± 1.23^{e}

[j]The result is expressed as a mean ± SD of three trials (n = 3). Statistical analysis was done by one-way analysis of variance (ANOVA) using the CoStat computer program accompanied by Tukey multiple comparison test at $p < 0.05$. Unshared superscript letters are significant values between groups at $p < 0.05$.

commonly found in marine algae, and previously identified in the brown algae *Ascophyllum nodosum*, *Fucus*, and *Laminaria*.[34]

A considerable number of fatty acid peaks were recorded in the second half of the chromatographic run, most of which are reported for the first time in *J. rubens*. A different profile of free fatty acids was determined showing a higher proportion of saturated fatty acids, while short-chain fatty acids were not detected. Two unsaturated long-chain fatty acids were identified in the LC-MS analysis. An unsaturated hydroxy fatty acid was identified at *m*/*z* 323.22 (Rt = 14.89 min), with a prominent product ion at *m*/*z* 305 due to the loss of a water molecule in its MS/MS spectrum, along with two diagnostic product ions at *m*/*z* 279 and 240, due to losses of CO_2 and $2H_2O$, respectively, characteristic of hydroxy fatty acids along with other ions at *m*/*z* 197 and 183. Based on product ions, peak 8 was annotated as hydroxyeicosadienoic acid. Similarly, another deprotonated ion at *m*/*z* 265.15 (Rt =16.57min) in peak 9 was identified as unsaturated fatty acid based on its two consecutive losses of H_2O and CO_2 yielding product ions at *m*/*z* 239 and 221, respectively, and annotated as heptadecadienoic acid, a C17 unsaturated fatty acid.

Saturated long-chain fatty acids were detected in peaks 7 and 10 from molecular ions *m*/*z* at 242.18 and *m*/*z* 297.15. Peak 7 yielded two product ions at *m*/*z* 225 and 198 due to the loss of H_2O and CO_2, respectively assigning it as pentadecanoic acid ($C_{15}H_{30}O_2$). Peak 10 similarly showed characteristic losses of fatty acids (H_2O and CO_2) to yield respective product ions at *m*/*z* 279 and 253, respectively, along with product ions at *m*/*z* 239, 197, and 170 assigning it as nonadecanoic acid. A deprotonated ion at *m*/*z* 311.17 showed product ions at *m*/*z* 293 and 267 due to neutral losses of H_2O and CO_2, respectively, in addition to characteristic fragment ions *m*/*z* 254, 239, 225, and 212 due to successive loss of CH_2 annotated as arachidic acid, $C_{20}H_{40}O_2$. Similarly, molecular ions *m*/*z* 325.18 (peak 12) and 339.20 (peak 13) showed a similar MS/MS fragmentation pattern to that of *m*/*z* 311.17 (*m*/*z* 239, 225, 197,183, and 170), with a characteristic mass difference of 14 and 28 Da, respectively. Fatty acid esterification is confirmed by the presence of the prominent product ion at *m*/*z* 296 in each MS/MS spectrum of peaks 12 and 13, indicating the loss of [M-OCH_2-H]- and [M-OC_2H_5-H]-, respectively and annotated as methyl and ethyl esters of arachidic acid, respectively. The later elution of these peaks compared to arachidic acid is due to their lower polarity.

2.3. Characterization of JCNP. *2.3.1. Particle Size (PS), ζ Potential (ZP), Polydispersity Index (PDI), and Encapsulation Efficiency (EE %).* JCNP must be small enough to control the release of the extract from the NP in drugs/supplements/food systems and inside the human body.[35] The PS of JCNP ranged from 161 to 669 nm (Table 3). Increasing both CS and TPP

https://doi.org/10.1021/acsomega.1c05517
ACS Omega 2022, 7, 6539−6548

concentrations was associated with a decrease in the PS, i.e., from (F1) to (F3) having PSs of 338 and 161 nm. However, further increase in CS/TPP concentrations led to an increase in PS to reach up to 669 (F6). The JCNP with the smallest PS were obtained for chitosan/TPP weights of 0.025 and 0.01 mg, respectively. Below this composition, the concentration of CS was insufficient to form cross-linked matrices with TPP. The PS of F3 decreased due to an increased density of cross-linking between CS and TPP.[36] Higher CS and TPP concentrations led to bigger PS due to the accumulation of the CS on the NP.[37] In addition, increasing the TPP concentration led to an enlargement in the PS due to aggregation of TPP on the NP, i.e., TPP has five negative groups that interact with the $-NH_3^+$ of the CS; thus, the PS enlargement could be due to higher exposure of anionic groups produced from increased TPP above the equilibrium.[20] Additionally, the excess availability of TPP could cause the inter/intramolecular cross-linkages to be associated with TPP facilitating the JCNP to be a form of big aggregates.[38] Furthermore, CS approaches the limit of a critical concentration of coil overlap when its concentration is increased. Consequently, the CS chains are close to one another, they start forming connected coils, and then the TPP interacts with a minute amount of CS. Then, the CS molecules start folding over themselves.[39] Increasing the CS concentration increases the viscosity of the entire solution, which then decreases the diffusion of TPP producing large JCNP.[39] Alamdaran et al.[40] observed that at higher concentrations of CS, the interchain hydrogen bonds became more dominant and the PS increased. By increasing the TPP above the critical concentration, the cross-linking agent started occupying most of the positively charged -NH_3^+ of CS reducing the ZP and decreasing the electrostatic repulsion between the CS NP. Then, NP started aggregating forming large particles.

As presented in Table 3, the ZP of the NP ranged from +17.0 ± 8.91 to +31.2 ± 0.87 mV indicating the production of JCNP with good physical stability. The positive value of the ZP was due to the presence of CS -NH_3^+ groups. There was no significant difference between the ZP of all prepared formulae indicating that none of the varied compositions (CS and TPP weights) or conditions (HT and HS) influenced the ZP of JCNP. The PDI of JCNP varied from 0.139 ± 0.01 to 0.376 ± 0.01 (Table 3) indicating an acceptable particle size distribution and a reproducible method of nanoformulation.[20] There was no significant difference among the PDI values of all prepared formulae indicating that none of the varied compositions or conditions influenced the PDI.

The EE % of JCNP ranged from 60% ± 8.64 to 97% ± 4.87 indicating that the *J. rubens* algal extract was efficiently entrapped into the CS TPP NP (Table 3). Due to the freely available $-NH_3^+$ groups, CS carries a positive charge, and an electrostatic attraction takes place with the phytochemicals (negatively charged) augmenting the EE%.[41,42] Increasing both CS and TPP concentrations was associated with a significant increase in the EE %, i.e., from (F1) to (F3) having EE % of 60% ± 9.76 and 97% ± 4.87, respectively. However, a further increase in CS:TPP concentrations led to a decrease in EE % to reach 60% ± 8.64 (F6) due to an increased viscosity caused by the CS, which caused a decrease in the diffusion of the *J. rubens* extract inside the NP.[39] It was also revealed that a high CS concentration restricted the phytochemicals' cargo into CS matrices, possibly due to decreasing ionic interactions between CS and TPP.[43] As the TPP concentration increased, the EE % increased. This was possibly due to an elevated cross-linking of TPP capable of entrapping various phytochemicals and bioactive compounds.[44] Nonetheless, at a very high TPP concentration, the EE % was observed to decrease, possibly because of particle shrinkage. In other words, the very high level of cross-linkages led to the squeezing out of the phytochemicals from the NP causing the EE % to decrease.[20,39] By increasing the HT (F13), the EE % decreased because higher HT caused the leakage of phytochemicals from the chitosan-TPP matrices.[45] Moreover, an increase in the HS led to higher EE %, followed by a gradual decrease in the encapsulation: at higher speed values, the EE % was high due to the augmentation of the cross-linkages among the CS and the phytochemicals. This could be due to the excessive potency of CS to produce ionic gels at elevated HS, which averts the leakage of the bioactive compounds to the external phase causing an enhanced EE %.[46] However, for F10 and F13, the EE % of JCNP decreased, probably due to the diffusion of the entrapped bioactive compounds to the external phase, causing a decrease in PS after operating a high HS.[47] To clarify, an increase in the speed decreased the JCNP size due to the fact that elevated HS decreases particle aggregation and progress cavitational forces in the homogenization gap. Accordingly, a reduction in the polymer size occurred with a succeeding decline in the EE % of the prepared JCNP.[48]

2.3.2. Scanning Electron Microscopy (SEM). JCNP were homogeneous in shape and exhibited smooth surfaces and uniform size distribution, as analyzed by SEM (Figure 2). This

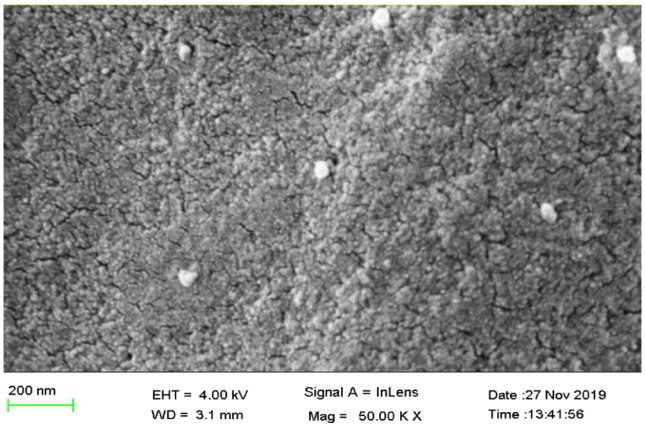

Figure 2. SEM Micrograph of JCNP.

result is in accordance with the micrographs obtained after encapsulation of chlorogenic acid into CS NPs.[49] The size ranges obtained by the SEM micrographs were smaller than the z-averages obtained by means of the Zetasizer, where a hydrodynamic diameter is being observed.[41]

2.3.3. In Vitro Release Study. The *in vitro* phytochemicals' release profiles of JCNP in comparison to the raw algal extract as a function of time are illustrated in Figure 3A,B. For the PBS intestinal fluid stimulation, JCNP showed a slow and sustained release of the phytochemicals throughout the run time, and a total of 92.6 ± 0.40% of the phytochemicals was released after 72 h (Figure 3 A). This compared with 77.6 ± 2.65% for the raw extract in the first 6 h indicates a burst release. The prolonged phytochemical release achieved by the formulated JCNP could be due to the delayed dissociation of the phytochemical molecules from the ionic binding between the cationic groups in the CS and the anionic groups in the *J. rubens* extract.[50] For the gastric fluid stimulation medium

https://doi.org/10.1021/acsomega.1c05517
ACS Omega 2022, 7, 6539−6548

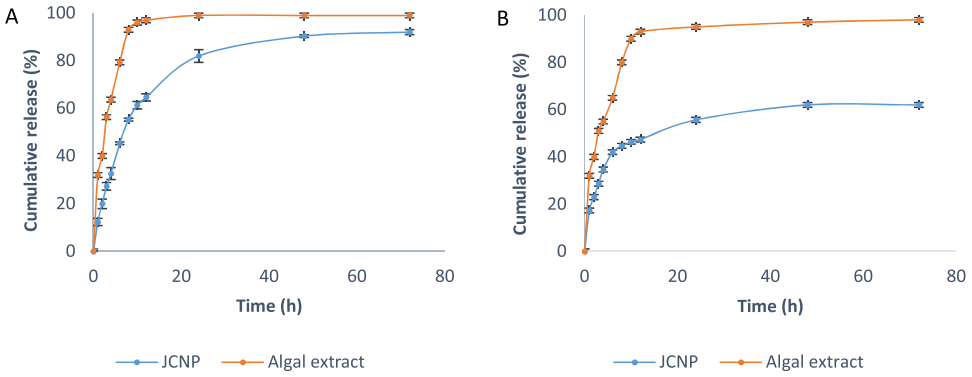

Figure 3. *In vitro* antioxidants' release from the optimal JCNP and the raw algal extract in (A) intestinal fluid stimulation media, pH 7.4, and in (B) gastric fluid stimulation media, pH 1.4. The result is expressed as a mean ± SD of three trials (n = 3).

(Figure 3B), JCNP showed a slow and a sustained release, with 62.9 ± 0.70% of the entrapped phytochemicals released after 72 h, as compared with 65.6 ± 60.6% for the raw extract in the first 6 h, which also indicates a burst release.

The release of the phytochemicals from JCNP followed a biphasic pattern. An initial fast release during the first 5 h was observed followed by a sustained phytochemicals' release over a period of 72 h. During the first 5 h, it was observed that the release rate of the phytochemicals was both slower and less in the intestinal fluid medium than that in the gastric stimulation medium. This was due to the fact that as the pH value decreased, the protonated groups of both the NP and the entrapped phytochemicals repelled each other resulting in the swelling of the entire system and the release of the phytochemicals. On the other hand, as the pH value increased, the electrostatic repulsion also decreased, and accordingly, the release became slower.[51] In the intestinal fluid stimulation, a higher release (92.6 ± 0.40%) was observed after 72 h as compared to that obtained in the gastric stimulation media (62.9 ± 0.70%) because CS is a weak polybase with a pK_a value of 6.3.[52] With increasing pH, the ionization of amine groups decreased; thus, the cross-linking density between CS and TPP at pH 7.4 was lower than that at pH 1.4, leading to a higher phytochemical release from the JCNP at pH 7.4. The results indicate a sustained release suggesting that the prepared JCNP could be a good choice for oral administration of the phytochemicals.

3. CONCLUSIONS

Algal phytochemicals were extracted from the red algal species *J. rubens* matrices by ethanol. Several antioxidant assays were carried out to ensure that the algal extract exhibits a potent antioxidant activity. Several secondary metabolites possessing an antioxidant activity were identified by means of chromatographic techniques of polar and nonpolar nature. Ionic gelation was successfully used to prepare JCNP with a PS of 161 nm, a ZP of 31.2 mV, a PDI of 0.211, and an EE % of 99.7%. The nanoencapsulation of the algal extract led to a sustained release in both the gastric and the intestinal simulation media. This indicates the potential advantages of encapsulated *J. rubens* extract, with its potent antioxidant activity, for use in different applications where sustained release is useful.

4. MATERIALS AND METHODS

4.1. Materials. Low molecular weight chitosan, sodium tripolyphosphate, diphenyl-2-picryl-hydrazyl reagent, Folin–Ciocalteu reagent, quercetin, 2,4,6-tripyridyl-*S*-triazine, and trolox were purchased from Sigma-Aldrich Chemical Co. (St. Louis). (*Z*)-3-hexenylacetate was purchased from Sigma Aldrich (Germany). All other chemicals were of pure analytical grade.

4.2. Sampling of *J. rubens* and Extraction of Phytochemicals. *4.2.1. Sampling of Algae.* The red algae *J. rubens* (rhodophyta) was freshly collected from the rocky bay of Abu-Qir (Alexandria, Egypt) at a depth of ca. 3.5 m. The algae were transferred to the lab in seawater and were then washed thoroughly with running water to remove the epiphytic/extraneous matter followed by rinsing with distilled water. *J. rubens* was then air-dried in the dark for 48 h to prevent the degradation of the bioactive compounds and stored in the dark at room temperature in evacuated polyethylene plastic bags until solvent extraction.[53]

4.2.2. Extraction of Bioactive Compounds. The *J. rubens*' bioactive compounds were extracted by suspending (20 g) clean and dry finely ground algal powder (i.e., ground in an electric mixer) in 300 mL of ethanol. The mixture was shaken for 48 h at room temperature using a water bath shaker set at 200 rpm. The supernatant was filtered twice using Whatman filter paper number 1. The filtrate was evaporated using a rotary evaporator at room temperature to yield a dry/gummy extract, which was stored at a temperature of −80 °C until further analysis.[54]

4.3. Total Phenolic/Flavonoid Contents and Antioxidant Assays. *4.3.1. TPC.* TPC was determined using the Folin–Ciocalteu method with minor modifications.[55] Gallic acid was used as a standard for the determination of total phenolics.[7] Different gallic acid dilutions (1, 2.5, 5, 10, 25, 50, and 100 μg/mL) at 1 mL aliquots were mixed with 5 mL of 10-fold diluted Folin–Ciocalteu reagent and 4 mL of Na_2CO_3 solution (7.5% w/v).[56] Likewise, 1 mL sample of the algal extract prepared at 1000 μg/mL was mixed with 5 mL of the Folin–Ciocalteu reagent, and 4 mL of Na_2CO_3 were added. The reaction mixture was incubated at room temperature for a duration of 1 h and then absorbance was measured at λ_{max} of 765 nm[57] against a blank prepared as above but without the algal extract.[58] TPC was expressed as mg GAE/g dry extract using the gallic acid calibration curve. All measurements were conducted in triplicate and expressed as mean ± SD.

4.3.2. TFC. TFC was determined according to the methods followed by Zhishen et al.[59] and Lin et al.,[60] with minor modifications. The *J. rubens*' ethanolic extract (0.5 mL) at a concentration of 0.1 g extract in 1 mL ethanol was first mixed

https://doi.org/10.1021/acsomega.1c05517
ACS Omega 2022, 7, 6539−6548

with 2 mL distilled water, followed by the addition of 0.15 mL of 5% (w/v) sodium nitrite and, after 5 min, 0.15 mL of 10% (w/v) aluminum chloride dissolved in distilled water was added. After a further 5 min, 2 mL (1 M) of sodium hydroxide was added. The absorbance of the mixture was then measured at λ_{max} of 510 nm[61] against deionized water as a blank. Quercetin was used to construct a standard calibration curve at dilutions of 1−50 μg/mL.[62] TFC was expressed as mg QE/g dry extract using the quercetin calibration curve. All measurements were conducted in triplicate and expressed as mean ± SD.

4.3.3. DPPH Assay. The DPPH assay was carried out to determine the *J. rubens' algal* extract capacity to free radical scavenging.[63] DPPH (0.0040 g) was dissolved in 100 mL of absolute ethanol to obtain a 40 ppm solution. Then, 2 mL of this solution was added to 2 mL of the algal extract at different concentrations, namely 50, 100, 250, 500, and 1000 μg/mL, followed by shaking. The mixture was left to stand in the dark at room temperature for a duration of 1 h. Decolorization of the DPPH• solution was determined by measuring the absorbance at λ_{max} of 517 nm[57] against absolute ethanol that was used as a blank.[64] DPPH was expressed in terms of radical scavenging activity (% RSA) and in terms of the half-maximal scavenging concentration (SC50) value. All the measurements were conducted in triplicate and expressed as mean ± SD.

4.3.4. FRAP Assay. The FRAP assay is based on the reduction of a ferric-tripyridyltriazine complex to its ferrous blue-colored form in the presence of antioxidants.[65] The FRAP reagent used contained 5 mL of a TPTZ (2,4,6-tripyridyl-S-triazine) solution (10 mmol/L) in HCl (40 mmol/L) plus 5 mL of $FeCl_3$ (20 mmol/L), and 50 mL of acetate buffer (0.3 mol /L, pH 3.6). The solution was freshly prepared and warmed to 37 °C. About 0.2 mL of seaweed (0.1 g/10 mL ethanol) was mixed with 1.8 mL of the FRAP reagent, and the absorbance of the reaction mixture was measured at λ_{max} of 593 nm[65] against distilled water as a blank after incubation at a temperature of 37 °C for 10 min. A standard curve was constructed using a Trolox solution.[66] The FRAP assay was expressed in terms of mg trolox/g dry weight of the extract. All of the measurements were conducted in triplicate and expressed as mean ± SD.

4.4. Chromatographic Analyses of the *J. rubens* Extract. *4.4.1. GC-MS.* GC-MS analysis was performed using an Agilent GC-MS5975C GC unit with a Triple-Axis Detector equipped with an autosampler. The GC column used was fused with a silica capillary column (length 30 m × diameter 0.25 mm × film thickness 0.25 μm) with helium as a carrier gas set at 1.5 L/min flow rate. The mass spectrometer was operated in the electron impact mode at 70 eV in the scan range of 40−700*m*/*z*. The split ratio was adjusted to 1:10, and the injected volume was 1 μl. The injector temperature was 250 °C, and the oven temperature was kept at 70 °C for 3 min and increased to 250 °C at 14 °C/min. For derivatization, 50 μL of methoxyamine hydrochloride in pyridine (20 mg/mL) was added as a first derivatizing agent. The mixture was incubated at 60 °C for 45 min. As the second derivatizing agent, 100 μL of *N*-methyl-*N*-(trimethylsilyl)-trifluoroacetamide (MSTFA) was added and incubated at 60 °C for 45 min. Peak identification was based on retention indices (RIs) relative to n-alkanes (C6−C20), and the mass spectra obtained were compared with those available in NIST libraries (NIST 11 - Mass Spectral Library, 2011 version) with an acceptance criterion of a match factor of ≥800.[67]

4.4.2. LC-MS. *The J. rubens* algal extract was chromatographically separated using an Acquity UPLC system (Waters Corp., Milford, MA) with an HSS T3 column (100 × 1.0 mm^2, particle size, 1.8 μm; Waters). The following conditions were applied: a binary gradient elution at a flow rate of 150 μL/min (0 to 1 min), isocratic 95% A (water/formic acid, 99.9:0.1 v-v), and 5% B (acetonitrile/formic acid, 99.9:0.1 v-v); 1 to 16 min, linear from 5 to 95% B; 16 to 18 min, isocratic 95% B; and 18 to 20 min, isocratic 5% B. The injection volume was a full loop (3.1 μL). A Micro TOF-Q hybrid quadrupole time-of-flight mass spectrometer (Bruker Daltonics Inc., Billerica, MA) was used for the detection of eluted compounds at *m*/*z* 100−1000, equipped with an Apollo-II electrospray ion source in positive and negative ion modes using the following instrument settings: nebulizer gas, nitrogen, 1.6 bar; dry gas, nitrogen, 6 L/min, 190 °C; capillary, −5500 V (+4000 V); endplate offset, −500 V; funnel 1 resolve filter (RF), 200 V peak to peak (Vpp); funnel 2 RF, 200 Vpp; in-source CID energy, 0 V; hexapole RF, 100 Vpp; quadrupole ion energy, 5 eV; collision gas, argon; collision energy, 10 eV; collision RF 200:400 Vpp (timing 50:50); transfer time, 70 μs; prepulse storage, 5 μs; pulse frequency, 10 kHz; and spectra rate, 3 Hz. Electrospray ionization-tandem mass spectrometry (ESI-MSn) spectra were obtained using a UPLCQ Deca XP MAX system (Thermo-Electron Co., San Jose, CA) equipped with an ESI source (electrospray voltage, 4.0 kV; sheath gas, nitrogen; capillary temperature, 275 °C) in positive and negative ionization modes. The Ion Trap MS system was coupled with the same Waters UPLC setup, using the same elution gradient system. The MS spectra were obtained during the UPLC run using the following conditions: MS/MS analysis with a starting collision-induced dissociation energy of 20 eV and an isolation width of +2 amu in data-dependent positive and negative ionization modes. Metabolites were characterized by their UV−vis spectra (220−600 nm) derived using a Dionex ICS−Series PDA Photodiode Array Detector (Thermo Fisher Scientific), mass spectra and comparison to an in-house database, Mass Bank, http://www.massbank.jp/ and the Dictionary of Natural Products.[68]

4.5. Preparation and Characterization of JCNP. *4.5.1. Nanoencapsulation of the J. rubens Extract by Ionic Gelation.* Dissimilar JCNP formulations were produced by means of an ionic gelation technique using TPP as the cross-linking agent.[39] A quantity of 0.005 g extract of *J. rubens* was dissolved in ethanol (0.5 mL). Diverse weights of CS were dissolved in 9 mL of 1% (v/v) acetic acid, and the pH was adjusted at 4. Then, 0.5 mL from the freshly prepared algal solution was added to the CS solution. The mixture was stirred at a speed of 600 rpm for a duration of 15 min. Different weights of TPP were dissolved in distilled water. Then, 1 mL of the TPP solution was added dropwise to the prepared solution throughout homogenization by means of a high-pressure homogenizer at diverse speeds and for varied durations (UltraTurrax T-25, IKA, Germany). The prepared JCNP were separated by means of centrifugation (Sigma Laborzentrifugen 1−14, Germany) at a speed of 18 000 rpm (equivalent to 36 288 g) for a duration of 20 min.[20,39] Table 4 shows the different compositions and conditions of the prepared formulae. All data were expressed as mean ± SD of three replicates in each formula. Statistical analysis was carried out by one-way analysis of variance (ANOVA), CoStat Software Computer Program accompanied with Tukey multi-

https://doi.org/10.1021/acsomega.1c05517
ACS Omega 2022, 7, 6539−6548

Table 4. Preparation Conditions of Different JCNP

formula	CS (g)	TPP (g)	HT (min)	HS (rpm)
F1	0.010	0.004	5	12
F2	0.020	0.008	5	12
F3	0.025	0.010	5	12
F4	0.030	0.012	5	12
F5	0.040	0.015	5	12
F6	0.050	0.015	5	12
F7	0.025	0.010	3.5	9
F8	0.025	0.010	6	12
F9	0.025	0.010	5	15
F10	0.025	0.010	5	18
F11	0.025	0.010	7	12
F12	0.025	0.010	7	15
F13	0.025	0.010	9	18

ple comparison tests where unshared letters are significant at $P < 0.05$.

4.5.2. PS/PDI Analysis and the ZP Measurement of JCNP. The PS and PDI were measured by dynamic light scattering using a Zetasizer (Malvern Instrument Ltd., Worcestershire, U.K.) operating with a 633 nm laser at 25 °C with an angle of detection of 173°. The electrophoretic mobility measurements were performed at 25 °C for 120 s using a combination of laser Doppler velocimetry and phase analysis light scattering. All measurements were performed in triplicate, and the results were reported in terms of PD/PDI/ZP ± SD.

4.5.3. Determination of EE % of JCNP. The EE % of JCNP was measured from the clear solution obtained after separation of the free algal extract from JCNP by centrifugation at 18 000 rpm (equivalent to 36288 g) for 20 min. The amount of free *J. rubens* was estimated with a UV−vis spectrophotometer (CARY 500 SCAN Varian, Hi-tech) at λ_{max} of 658 nm by comparing the absorbance to a preconstructed calibration curve ($r^2 = 1$, $n = 3$). The EE % was calculated according to the following equation

$$\text{EE\%} = \frac{(\text{total extract added} - \text{free extract in supernatant})}{\text{total extract added}} \times 100$$

4.5.4. Morphological Examination. The surface morphology, shape, and size of JCNP were examined using an SEM (Zeiss, Leo Supra 55 FE). A lyophilized JCNP sample was fixed with a double-sided adhesive tape on the SEM sample holder. The specimen was then coated with gold using a sputter coater under argon atmosphere to achieve a 150 Å thick film.[69]

4.5.5. In Vitro Release Assay. The *in vitro* phytochemicals' release from JCNP and the raw extract was studied by the dialysis bag diffusion method.[70] Aliquots of 2 mL of the optimum JCNP, each equivalent to 1 mg of the algal extract, were dispersed in dialysis bags, each with 20 mL of phosphate buffer saline (PBS) as an intestinal fluid simulation medium with a pH of 7.4,[71] and in bags each with 20 mL of 0.1 M HCl buffer as a gastric fluid simulation medium with a pH of 1.4 (HCl does not totally mimic the gastric juice).[58] This was also carried out for portions of the pure algal extract, each of 1 mg, subjected to the same conditions as the JCNP samples. The solutions were stirred at a speed of 50 rpm with the temperature maintained at 37 ± 1 °C. At specific time intervals of 0, 1, 2, 3, 4, 6, 8, 10, 12, 24, 48, and 72 h, 2 mL of each of the medium were withdrawn from outside the dialysis bags and replaced with equal amounts of fresh PBS and 0.1 M HCl, respectively. Samples were analyzed by a UV−visible spectrophotometer (CARY 500 SCAN Varian, Hi-tech) at λ_{max} of 658 nm. Triplicate samples were analyzed for each measurement, and the mean cumulative release ± SD was determined.[72]

■ ASSOCIATED CONTENT

Supporting Information

The Supporting Information is available free of charge at https://pubs.acs.org/doi/10.1021/acsomega.1c05517.

% Radical scavenging activity and % remaining DPPH of the *J. rubens* extract (Figure S1); *Jania rubens* is a red petrified seaweed species; its height ranges from 15 to 40 cm; *Jania rubens* has pink fronds that are composed of rounded bunches and has a thallus whose fronds are rigid and joined with very thin branches (PDF)

■ AUTHOR INFORMATION

Corresponding Author

Yasmin R. Maghraby − *Chemistry Department, The American University in Cairo, New Cairo 11835, Egypt;* orcid.org/0000-0003-1152-4777; Email: ymaghraby@aucegypt.edu

Authors

Mohamed A. Farag − *Chemistry Department, The American University in Cairo, New Cairo 11835, Egypt; Pharmacognosy Department, College of Pharmacy, Cairo University, Cairo 11562, Egypt;* orcid.org/0000-0001-5139-1863

Michael G Kontominas − *Department of Chemistry, University of Ioannina, Ioannina 45110, Greece*

Zeinab T. Shakour − *Pharmacognosy Department, National Center for Natural Products Research, Giza 11111, Egypt*

Adham R. Ramadan − *Chemistry Department, The American University in Cairo, New Cairo 11835, Egypt*

Complete contact information is available at: https://pubs.acs.org/10.1021/acsomega.1c05517

Notes

The authors declare no competing financial interest.

■ ACKNOWLEDGMENTS

Y.R.M. wishes to thank the American University in Cairo for the financial support.

■ ABBREVIATIONS USED

CS, chitosan; **DPPH**, 2,2-diphenyl-1-picrylhydrazyl; **EE %**, encapsulation efficiency; **FRAP**, ferric reducing antioxidant power; **GAE**, gallic acid equivalents; **GC-MS**, gas chromatography-mass spectrometry; **GRAS**, generally recognized as safe; **HT**, homogenization time; **HS**, homogenization speed; **IC_{50}**, half-maximal inhibitory concentration; ***J. rubens***, *Jania rubens*; **JCNP**, *Jania rubens* chitosan nanoparticles; **KI**, Kovats index; **LC-MS**, liquid chromatography-mass spectrometry; **NP**, nanoparticles; **PBS**, phosphate buffer saline; **PDI**, polydispersity index; **PS**, particle size; **QE**, quercetin equivalents; **RSA**, radical scavenging activity; **RT**, retention time; **SEM**, scanning electron microscopy; **TFC**, total flavonoid content; **TPC**, total phenolic content; **TPP**, sodium tripolyphosphate; **ZP**, ζ potential

https://doi.org/10.1021/acsomega.1c05517
ACS Omega 2022, 7, 6539−6548

REFERENCES

(1) Shahidi, F.; Zhong, Y. Measurement of antioxidant activity. *J. Funct. Foods* **2015**, *18*, 757−781.
(2) Kelman, D.; Posner, E. K.; McDermid, K. J.; Tabandera, N. K.; Wright, P. R.; Wright, A. D. Antioxidant activity of Hawaiian marine algae. *Mar. Drugs* **2012**, *10*, 403−416.
(3) Devi, K. P.; Suganthy, N.; Kesika, P.; Pandian, S. K. Bioprotective properties of seaweeds: *In vitro* evaluation of antioxidant activity and antimicrobial activity against food borne bacteria in relation to polyphenolic content. *BMC Complement Altern. Med.* **2008**, *8*, No. 38.
(4) Kamil, A.; Chen, C. Y. O.; Blumberg, J. B. The application of nanoencapsulation to enhance the bioavailability and distribution of polyphenols. *Nanotechnol. Funct. Foods.* **2015**, *14*, 158−174.
(5) Scalbert, A.; Williamson, G. Dietary Intake and Bioavailability of Polyphenols. *J. Nutr.* **2000**, *130*, 2073−2085.
(6) Ibrahim, A. M. M.; Mostafa, M. H.; El-Masry, M. H.; El-Naggar, M. M. A. Active biological materials inhibiting tumor initiation extracted from marine algae. *Egypt. J. Aquat. Res.* **2005**, *31*, 146−156.
(7) Chakraborty, K.; Joseph, D.; Praveen, N. K. Antioxidant activities and phenolic contents of three red seaweeds (Division: Rhodophyta) harvested from the Gulf of Mannar of Peninsular India. *J. Food Sci. Technol.* **2015**, *52*, 1924−1935.
(8) Ahmed, H. H.; Hegazi, M. M.; Abd-Alla, H. I.; Eskander, E. F.; Ellithey, M. S. Antitumour and antioxidant activity of some red sea seaweeds in Ehrlich ascites carcinoma in vivo. *Z. Naturforsch. C. J. Biosci.* **2011**, *66*, 367−376.
(9) Fathi, M.; Varshosaz, J. Novel hesperetin loaded nanocarriers for food fortification: Production and characterization. *J. Funct. Foods.* **2013**, *5*, 1382−1391.
(10) Ohara, M.; Ohyama, Y. Delivery and application of dietary polyphenols to target organs, tissues and intracellular organelles. *Curr. Drug Metab.* **2014**, *15*, 37−47.
(11) Manach, C.; Scalbert, A.; Morand, C.; Rémésy, C.; Jiménez, L. Polyphenols: Food sources and bioavailability. *Am. J. Clin.Nutr.* **2004**, *79*, 727−747.
(12) Kamil, A.; Chen, C. Y. O.; Blumberg, J. B. The application of nanoencapsulation to enhance the bioavailability and distribution of polyphenols. *Nanotechnol. Funct. Foods.* **2015**, *14*, 158−174.
(13) Lu, W.; Kelly, A. L.; Miao, S. Emulsion-based encapsulation and delivery systems for polyphenols. *Trends Food Sci. Technol.* **2016**, *47*, 1−9.
(14) Dudhani, A. R.; Kosaraju, S. L. Bioadhesive chitosan nanoparticles: Preparation and characterization. *Carbohydr. Polym.* **2010**, *81*, 243−251.
(15) Hu, B.; Liu, X.; Zhang, C.; Zeng, X. Food macromolecule based nanodelivery systems for enhancing the bioavailability of polyphenols. *J. Food Drug Anal.* **2017**, *25*, 3−15.
(16) Jain, A.; Thakur, K.; Sharma, G. Polymeric nanoparticles containing diazepam: preparation, optimization, characterization, *in-vitro* drug release and release kinetic study. *Colloids Surf. B.* **2016**, *3*, 143−151.
(17) Ibrahim, H. M.; El-Bisi, M. K.; Taha, G. M.; El-Alfy, E. A. Chitosan nanoparticles loaded antibiotics as drug delivery biomaterial. *J. Appl. Pharm. Sci.* **2015**, *5*, No. 085-090.
(18) Wang, J. J.; Zeng, Z. W.; Xiao, R. Z. Recent advances of chitosan nanoparticles as drug carriers. *Int. J Nanomedicine* **2011**, *6*, 765−774.
(19) Tang, D. W.; Yu, S. H.; Ho, Y. C.; et al. Characterization of tea catechins-loaded nanoparticles prepared from chitosan and an edible polypeptide. *Food Hydrocoll.* **2013**, *30*, 33−41.
(20) Delan, W. K.; Zakaria, M.; Elsaadany, B.; ElMeshad, A. N.; Mamdouh, W.; Fares, A. R. Formulation of simvastatin chitosan nanoparticles for controlled delivery in bone regeneration: Optimization using Box-Behnken design, stability and in *vivo study*. *Int. J. Pharm.* **2020**, *577*, No. 119038.
(21) Ismail, M. M.; Gheda, S. F.; Pereira, L. Variation in bioactive compounds in some seaweeds from Abo Qir bay, Alexandria, Egypt. *Rend. Lincei.* **2016**, *27*, 269−279.
(22) Maqsood, S.; Benjakul, S.; Abushelaibi, A.; Alam, A. Phenolic compounds and plant phenolic extracts as natural antioxidants in prevention of lipid oxidation in seafood: A detailed review. *Compr. Rev. Food Sci. Food Saf.* **2014**, *13*, 1125−1140.
(23) Natrah, F. M. I.; Yusoff, F. M.; Shariff, M.; Abas, F.; Mariana, N. S. Screening of Malaysian indigenous microalgae for antioxidant properties and nutritional value. *J. Appl. Phycol.* **2007**, *19*, 711−718.
(24) Uluata, S.; Özdemir, N. Antioxidant activities and oxidative stabilities of some unconventional oilseeds. *J. Am. Oil Chem. Soc.* **2012**, *89*, 551−559.
(25) Polat, S.; Ozogul, Y. Seasonal proximate and fatty acid variations of some seaweeds from the northeastern Mediterranean coast. *Oceanologia* **2013**, *55*, 375−391.
(26) Abdel-raouf, N.; Borie, I.; Ibraheem, M. *In vivo* application of *Jania rubens* silver nanoparticles as chemopreventive. *Aus. J Basic App. Sci.* **2017**, *11*, 176−186.
(27) Abdel-Latif, H. H.; Shams El-Din, N. G.; Ibrahim, H. A. H. Antimicrobial activity of the newly recorded red alga *Grateloupia doryphora* collected from the Eastern Harbor, Alexandria, Egypt. *J. Appl. Microbiol.* **2018**, *125*, 1321−1332.
(28) Cikman, O.; Soylemez, O.; Ozkan, O. F.; et al. Antioxidant activity of syringic acid prevents oxidative stress in l-arginine-induced acute pancreatitis: An experimental study on rats. *Int. Surg. J.* **2015**, *100*, 891−896.
(29) Govindappa, M.; Prathap, S.; Vinay, V.; Channabasava, R. Chemical composition of methanol extract of endophytic fungi, alternaria sp. of tebebuia argentea and their antimicrobial and antioxidant activity. *Int. J. Biol. Pharm. Res.* **2014**, *5*, 861−869.
(30) Welling, M.; Ross, C.; Pohnert, G. A desulfatation-oxidation cascade activates coumarin-based cross-linkers in the wound reaction of the giant unicellular alga *dasycladus vermicularis*. *Angew. Chem., Int. Ed.* **2011**, *50*, 7691−7694.
(31) Bailly, F.; Maurin, C.; Teissier, E.; Vezin, H.; Cotelle, P. Antioxidant properties of 3-hydroxycoumarin derivatives. *Bioorg. Med. Chem.* **2004**, *12*, 5611−5618.
(32) Zhong, B.; Robinson, N. A.; Warner, R. D.; Barrow, C. J.; Dunshea, F. R.; Suleria, H. A. R. LC-ESI-QTOF-MS/MS characterization of seaweed phenolics and their antioxidant potential. *Mar. Drugs* **2020**, *18*, No. 331.
(33) Cornish, M. L.; Garbary, D. J. Antioxidants from macroalgae: potential applications in human health and nutrition. *Algae* **2010**, *25*, 155−171.
(34) MacKinnon, S. L.; Hiltz, D.; Ugarte, R.; Craft, C. A. Improved methods of analysis for betaines in *Ascophyllum nodosum* and its commercial seaweed extracts. *J. Appl. Phycol.* **2010**, *22*, 489−494.
(35) McClements, D. J. Encapsulation, protection, and release of hydrophilic active components: Potential and limitations of colloidal delivery systems. *Adv. Colloid Interface Sci.* **2015**, *219*, 27−53.
(36) Fan, W.; Yan, W.; Xu, Z.; Ni, H. Formation mechanism of monodisperse, low molecular weight chitosan nanoparticles by ionic gelation technique. *Colloids Surf. B.* **2012**, *90*, 21−27.
(37) Hu, B.; Pan, C.; Sun, Y.; et al. Optimization of fabrication parameters to produce chitosan-tripolyphosphate nanoparticles for delivery of tea catechins. *J. Agric. Food Chem.* **2008**, *56*, 7451−7458.
(38) Rampino, A.; Borgogna, M.; Blasi, P.; Bellich, B.; Cesàro, A. Chitosan nanoparticles: Preparation, size evolution and stability. *Int. J. Pharm.* **2013**, *455*, 219−228.
(39) Motawi, T. K.; El-Maraghy, S. A.; ElMeshad, A. N.; Nady, O. M.; Hammam, O. A. Cromolyn chitosan nanoparticles as a novel protective approach for colorectal cancer. *Chem. Biol. Int.* **2017**, *275*, 1−12.
(40) Alamdaran, M.; Movahedi, B.; Mohabatkar, H.; Behbahani, M. *In-vitro* study of the novel nanocarrier of chitosan-based nanoparticles conjugated HIV-1 P24 protein-derived peptides. *J. Mol. Liq.* **2018**, *265*, 243−250.
(41) Servat-Medina, L.; González-Gómez, A.; Reyes-Ortega.; et al. Chitosan−tripolyphosphate nanoparticles as Arrabidaea chica standardized extract carrier: Synthesis, characterization, biocompatibility,

https://doi.org/10.1021/acsomega.1c05517
ACS Omega 2022, 7, 6539−6548

and antiulcerogenic activity. *Int. J. Nanomedicine* **2015**, *10*, 3897−3909.
(42) Santos, T. C.; Hernández, R.; Rescignano, N.; et al. Nanocomposite chitosan hydrogels based on PLGA nanoparticles as potential biomedical materials. *Eur. Polym. J.* **2018**, *99*, 456−463.
(43) Shukr, M. H.; Ismail, S.; Ahmed, S. M. Development and optimization of ezetimibe nanoparticles with improved antihyperlipidemic activity. *J. Drug Sci. Technol.* **2019**, *49*, 383−395.
(44) Yadav, S. K.; Khan, G.; Bansal, M.; Vardhan, H.; Mishra, B. Screening of ionically crosslinked chitosan-tripolyphosphate microspheres using Plackett−Burman factorial design for the treatment of intrapocket infections. *Drug Dev. Ind. Pharm.* **2017**, *43*, 1801−1816.
(45) Abul Kalam, M.; Khan, A. A.; Khan, S.; Almalik, A.; Alshamsan, A. Optimizing indomethacin-loaded chitosan nanoparticle size, encapsulation, and release using Box-Behnken experimental design. *Int. J. Biol. Macromol.* **2016**, *87*, 329−340.
(46) Auwal, S. M.; Zarei, M.; Tan, C. P.; Basri, M.; Saari, N. Enhanced physicochemical stability and efficacy of angiotensin I-converting enzyme (ACE) - Inhibitory biopeptides by chitosan nanoparticles optimized using Box-Behnken design. *Sci. Rep.* **2018**, *8*, No. 10411.
(47) Patel, B. K.; Parikh, R. H.; Aboti, P. S. Development of Oral Sustained Release Rifampicin Loaded Chitosan Nanoparticles by Design of Experiment. *J. Drug Delivery* **2013**, *2013*, 1−10.
(48) Patil, P.; Bhoskar, M. Optimization and evaluation of spray dried chitosan nanoparticles containing Doxorubicin. *Int. J. Curr. Pharm. Res.* **2014**, *6*, 7−15.
(49) Nallamuthu, I.; Devi, A.; Khanum, F. Chlorogenic acid loaded chitosan nanoparticles with sustained release property, retained antioxidant activity and enhanced bioavailability. *Asian J. Pharm. Sci.* **2015**, *10*, 203−211.
(50) Kulhari, H.; Pooja, D.; Prajapati, S. K.; Chauhan, A. S. Performance evaluation of PAMAM dendrimer based simvastatin formulations. *Int. J. Pharm.* **2011**, *405*, 203−209.
(51) Anirudhan, T. S.; Dilu, D.; Sandeep, S. Synthesis and characterization of chitosan crosslinked-β-cyclodextrin grafted silylated magnetic nanoparticles for controlled release of Indomethacin. *J. Magn. Magn. Mater.* **2013**, *343*, 149−156.
(52) Yalpani, M.; Hall, L. D. Some chemical and analytical aspects of polysaccharide modifications.1 3. formation of branched-chain, soluble chitosan derivatives. *Macromolecules* **1984**, *17*, 272−281.
(53) Fleita, D.; El-Sayed, M.; Rifaat, D. Evaluation of the antioxidant activity of enzymatically-hydrolyzed sulfated polysaccharides extracted from red algae; *Pterocladia capillacea*. *LWT - Food Sci. Technol.* **2015**, *63*, 1236−1244.
(54) Balboa, E. M.; Conde, E.; Moure, A.; Falqué, E.; Domínguez, H. *In vitro* antioxidant properties of crude extracts and compounds from brown algae. *Food Chem.* **2013**, *138*, 1764−1785.
(55) Waterhouse, A. Folin-Ciocalteau micro method for total phenol in wine. *Wat. Lab.* **2012**, *13*, 1−3.
(56) Sharma, G. N.; Dubey, S. K.; Sati, N.; Sanadya, J. Phytochemical screening and estimation of total phenolic content in aegle marmelos seeds. *Int. J Pharm. Clin. Res.* **2011**, *3*, 27−29.
(57) Alam, M. N.; Bristi, N. J.; Rafiquzzaman, M. Review on *in vivo* and *in vitro* methods evaluation of antioxidant activity. *Saudi Pharm. J.* **2013**, *21*, 143−152.
(58) Chen, L.; Subirade, M. Chitosan/β-lactoglobulin core-shell nanoparticles as nutraceutical carriers. *Biomaterials* **2005**, *26*, 6041−6053.
(59) Zhishen, J.; Mengcheng, T.; Jianming, W. The determination of flavonoid contents in mulberry and their scavenging effects on superoxide radicals. *Food Chem.* **1999**, *64*, 555−559.
(60) Lin, J. Y.; Tang, C. Y. Determination of total phenolic and flavonoid contents in selected fruits and vegetables, as well as their stimulatory effects on mouse splenocyte proliferation. *Food Chem.* **2007**, *101*, 140−147.
(61) Gulati, V.; Harding, I. H.; Palombo, E. A. Enzyme inhibitory and antioxidant activities of traditional medicinal plants: Potential application in the management of hyperglycemia. *BMC Complement. Altern. Med.* **2012**, *12*, 1−9.
(62) Heiras-Palazuelos, M. J.; Ochoa-Lugo, M. I.; Gutiérrez-Dorado, R.; et al. Technological properties, antioxidant activity and total phenolic and flavonoid content of pigmented chickpea (Cicer arietinum L.) cultivars. *Int. J. Food Sci. Nutr.* **2013**, *64*, 69−76.
(63) Prabhasankar, P.; Ganesan, P.; Bhaskar, N.; et al. Edible Japanese seaweed, wakame (*Undaria pinnatifida*) as an ingredient in pasta: Chemical, functional and structural evaluation. *Food Chem.* **2009**, *115*, 501−508.
(64) Anagnostopoulou, M. A.; Kefalas, P.; Papageorgiou, V. P.; Assimopoulou, A. N.; Boskou, D. Radical scavenging activity of various extracts and fractions of sweet orange peel (Citrus sinensis). *Food Chem.* **2006**, *94*, 19−25.
(65) Hajimahmoodi, M.; Faramarzi, M. A.; Mohammadi, N.; Soltani, N.; Oveisi, M. R.; Nafissi-Varcheh, N. Evaluation of antioxidant properties and total phenolic contents of some strains of microalgae. *J. Appl. Phycol.* **2010**, *22*, 43−50.
(66) Katalinic, V.; Milos, M.; Kulisic, T.; Jukic, M. Screening of 70 medicinal plant extracts for antioxidant capacity and total phenols. *Food Chem.* **2006**, *94*, 550−557.
(67) Farag, M. A.; Fahmy, S.; Choucry, M. A.; Wahdan, M. O.; Elsebai, M. F. Metabolites profiling reveals for antimicrobial compositional differences and action mechanism in the toothbrushing stick "miswak" Salvadora persica. *J. Pharm. Biomed. Anal.* **2017**, *133*, 32−40.
(68) Mohsen, E.; Younis, I. Y.; Farag, M. A. Metabolites profiling of Egyptian *Rosa damascena* Mill. flowers as analyzed via ultra-high-performance liquid chromatography-mass spectrometry and solid-phase microextraction gas chromatography-mass spectrometry in relation to its anti-collagenase skin effect. *Ind. Crops Prod.* **2020**, *155*, No. 112818.
(69) Tiburu, E. K.; Salifu, A.; Aidoo, E. O.; et al. Formation of chitosan nanoparticles using deacetylated chitin isolated from freshwater algae and locally synthesized Zeolite A and their influence on cancer cell growth. *Nano Res.* **2017**, *48*, 156−170.
(70) Sessa, M.; Balestrieri, M. L.; Ferrari, G.; et al. Bioavailability of encapsulated resveratrol into nanoemulsion-based delivery systems. *Food Chem.* **2014**, *147*, 42−50.
(71) Luo, Y.; Zhang, B.; Cheng, W. H.; Wang, Q. Preparation, characterization and evaluation of selenite-loaded chitosan/TPP nanoparticles with or without zein coating. *Carbohydr. Polym.* **2010**, *82*, 942−951.
(72) Mitri, K.; Shegokar, R.; Gohla, S.; Anselmi, C.; Müller, R. H. Lutein nanocrystals as antioxidant formulation for oral and dermal delivery. *Int. J. Pharm.* **2011**, *420*, 141−146.

https://doi.org/10.1021/acsomega.1c05517
ACS Omega 2022, 7, 6539−6548